Computers Math. Applic. Vol. 25, No. 7, pp. 65–79, 1993
Printed in Great Britain.
0097-4943/93 $6.00 + 0.00

CONTINUATION-MINIMIZATION METHODS FOR STABILITY PROBLEMS

E. L. Allgower
Department of Mathematics, Colorado State University
Fort Collins, CO 80523, U.S.A.
C.-S. Chien*
Department of Applied Mathematics, National Chung-Hsing University
Taichung, Taiwan, 402, R.O.C.

(Received June 1992)

Abstract—We study the solution branches of stable and unstable bifurcations in certain semilinear elliptic eigenvalue problems with Dirichlet boundary conditions. A secant predictor-line search backtrack corrector continuation method is described to trace the solution curves numerically. Sample numerical results with computer graphic output are reported.

1. INTRODUCTION

Consider the following semilinear elliptic eigenvalue problems of the form

$$\begin{aligned} \Delta u + \lambda f(u) &= 0 \qquad \text{in } \Omega = [0,1]^2, \\ u &= 0 \qquad \text{on } \partial\Omega, \end{aligned} \tag{1.1}$$

where f is a smooth odd function which is normalized so that $f(0) = 0$, $f'(0) = 1$, $f''(0) = 0$ and $f'''(0) \neq 0$, and $\partial\Omega$ denotes the boundary of Ω. Since $f(0) = 0$, $u = 0$ is the trivial solution of (1.1). Nontrivial solutions of (1.1) branching from the bifurcation point $(0, \lambda_{m,n})$ on the trivial solution curve may be obtained either by the group theoretic methods or the Lyapunov-Schmidt methods on bifurcations, see [1,2] and the references cited therein. However, these two methods do not immediately furnish a means of differentiating between stable and unstable solutions.

In [3], Book *et al.* have investigated the solutions of

$$\begin{aligned} \Delta u + \lambda \sin hu &= 0 \qquad \text{in } \Omega = [0,1]^2, \\ u &= 0 \qquad \text{on } \partial\Omega, \end{aligned} \tag{1.2}$$

numerically, where some primary and secondary states were obtained. The physical meaning of (1.2) was also discussed therein.

Later, Budden and Norbury [4,5] reinvestigated the solutions of (1.1) both analytically and numerically by using $f(u) = \sin hu$ and $f(u) = u - u^3$ as two typical examples. After that, Allgower and Chien [6] and Chien [7] also gave some numerical reports concerning the primary and secondary states of $f(u) = \sin u$, respectively. Note that, for $f(u) = u - u^3$ and $f(u) = \sin u$, these two eigenvalue problems have the same qualitative solution structures.

Recently, Allgower *et al.* [1,2] have established the following result by using a modified Lyapunov-Schmidt method: At a corank ρ bifurcation point $(0, \lambda_0)$, (1.1) has eaxctly $(3^\rho - 1)/2$ different solution branches bifurcating from $(0, \lambda_0)$. Moreover, if $f'''(0) > 0$, these solutions are stable. Conversely, for $f'''(0) < 0$, these solutions are unstable. Thus, the total number of nontrivial solutions bifurcating from the trivial solution is completely determined, and the nodal

*Supported by the NSC of R.O.C. through Grant NSC 82-0208-M005-039.

Typeset by $\mathcal{A}_\mathcal{M}\mathcal{S}$-TEX lines of nontrivial solutions can be obtained. Therefore, one may exploit predictor-corrector continuation methods [6–12] and use local perturbation [6,7,11] for branch switching since the configurations of nontrivial solutions are known.

The purpose of this paper is twofold. First, we will describe a predictor-corrector continuation method to trace the solution curves of (1.1). A minimization method will be used as correctors, where the descent direction is provided by the GMRES, see [8,13–15]. Next, we will show the differences of the secondary states between stable and unstable bifurcations numerically. Our examples are $f(u) = \sinh u$ and $f(u) = \sin u$. Actually these two equations are qualitatively different.

This paper is organized as follows. In Section 2, we discuss the numerical continuation methods where a secant predictor-line search backtrack corrector algorithm is given. In order to extend the generality of this technique the basic theory and finite difference approximation of semilinear elliptic egienvalue problems with Neumann boundary conditions are described in Section 3. We remark here that the results also hold for Dirichlet boundary conditions. Our numerical results concering (1.1) are reported in Section 4. Again, similar computations can be executed on Neumann or mixed type boundary problems. Finally, some concluding remarks are given in Section 5.

2. NUMERICAL CONTINUATION METHODS

2.1. Basic Theory

In order to trace the solution curves of (1.1) numerically by the continuation methods, one may discretize it either by a finite difference or a finite element method. The finite dimensional approximation of (1.1) is then given by

$$H(x, \mu) = 0,$$

where $H : \mathbb{R}^{N+1} \to \mathbb{R}^N$ is a smooth mapping. Assume that 0 is a regular value of H. It is well known that $H^{-1}(0)$ is a 1-dimensional manifold which is the disjoint union of smooth curves $c(s)$ which are diffeomorphic to some interval $I \subset \mathbb{R}^1$ or to a circle S^1. We denote $c(s)$ by

$$c = \{y(s) = (x(s), \mu(s)) \mid H(y(s)) = 0,\ s \in I\}. \tag{2.1}$$

One may trace c via predictor-corrector continuation methods by solving the Davidenko initial value problem

$$\begin{aligned} &H'(y(s)) \cdot \dot{y}(s) = 0, \\ &\|\dot{y}(s)\| = 1, \\ &y(0) = (x(0), \mu(0)), \end{aligned} \tag{2.2}$$

where $H'(y(s)) = (D_x H(y(s)), D_\mu H(y(s)))$ is the $N \times (N+1)$ Jacobian matrix of rank N. In this case one solves the linear system of equations

$$Az = b, \tag{2.3}$$

where $b = \begin{bmatrix} \bar{0} \\ 1 \end{bmatrix}$ if a tangent vector is computed, and $b = \begin{bmatrix} -H(y) \\ 1 \end{bmatrix}$ if Newton corrector is performed, see, e.g., [6–10] for details. Here, $A = A(y(s))$ is the augmented Jacobian matrix defined by

$$A = \begin{bmatrix} H'(y(s)) \\ \dot{y}(s)^{\mathsf{T}} \end{bmatrix},$$

which is nonsingular for all $s \in I$. Note that in general A is nonsymmetric.

2.2. Nonlinear GMRES Corrector

Based on our numerical results in [9], the GMRES [15] or IGMRES [13] are very efficient linear solvers and can be incorporated in the context of continuation methods for solving nonlinear eigenvalue problems. First, we will discuss how nonlinear GMRES or IGMRES can be used as fast linear solvers for (2.3), wherein the Jacobian matrix is approximated by some difference quotients.

Let $H : \mathbb{R}^N \times \mathbb{R} \to \mathbb{R}^N$ be defined as above. We will solve $H(y) = 0$ by a secant predictor-GMRES corrector continuation method.

Suppose that y_{i-2}, y_{i-1} are two accepted approximating points to the solution curve c, where $H(c(s)) = 0$. The secant predictor is given by

$$y_i^{(0)} = y_{i-1} + h_{i-1} \cdot t_{i-1}. \tag{2.4}$$

Here, h_{i-1} is the current stepsize, and $t_{i-1} = (y_{i-1} - y_{i-2})/\|y_{i-1} - y_{i-2}\|$ is the secant direction. If we set $w_0 := y_i^{(0)}$, then from (2.3) we know that Newton corrector is performed by solving

$$\begin{bmatrix} H'(w_i) \\ t_{i-1}^{\mathrm{T}} \end{bmatrix} \cdot \delta_i = \begin{bmatrix} -H(w_i) \\ 0 \end{bmatrix}, \qquad i = 0, 1, 2, \ldots, \tag{2.5}$$

and then setting $w_{i+1} := w_i + \delta_i$ until convergence. The new approximating point y_i is obtained by setting $y_i = w_k$ for some positive integer k. Note that the tangent vector $\dot{y}_{i-1}(s)$ in (2.3) is replaced by the secant t_{i-1}.

For simplicity we rewrite (2.5) as

$$Az = b. \tag{2.6}$$

If $z^{(0)}$ is an initial guess for the true solution of (2.6), then letting $z = z^{(0)} + v$, we have the equivalent system

$$Av = r^{(0)},$$

where $r^{(0)} = b - Az^{(0)}$ is the initial residual. Let K_m be the Krylov subspace [14–16]

$$K_m \equiv \operatorname{span}\{r^{(0)}, Ar^{(0)}, \ldots, A^{m-1}r^{(0)}\},$$

GMERS finds an approximate solution

$$z^{(m)} = z^{(0)} + v^{(m)}, \qquad \text{with } v^{(m)} \in K_m,$$

such that

$$\|b - Az^{(m)}\|_2 = \min_{z \in z^{(0)} + K_m} \|b - Az\|_2 = \min_{v \in K_m} \|r_0 - Av\|_2. \tag{2.7}$$

The GMRES algorithm [15] is described as follows.

ALGORITHM 2.1. *GMRES*

(1) *Start: Choose an initial guess $z^{(0)}$ and a dimension m of the Krylov subspace.*
(2) *Arnoldi process:*
   (a) *Compute $r^{(0)} = b - Az^{(0)}$ and take $v_1 := r^{(0)}/\beta$ with $\beta = \|r^{(0)}\|_2$.*
   (b) *For $k = 1, 2, \ldots, m$ do*

$$\begin{aligned} \hat{v} &:= Av_k - \sum_{i=1}^{k} h_{i,k} v_i \quad \textit{with } h_{i,k} := (Av_k, v_i), \\ h_{k+1,k} &:= \|\hat{v}\|_2, \quad v_{k+1} := \frac{\hat{v}}{h_{k+1,k}}. \end{aligned} \tag{2.8}$$

(3) *Form the approximate solution: Define $\overline{H}_m$ to be the $(m+1) \times m$ Hessenberg matrix whose nonzero entries are the coefficients $h_{i,j}$, $1 \le i \le j+1$, $1 \le j \le m$, and define $V_m \equiv [v_1, v_2, \ldots, v_m]$.*
   (a) *Find the vector $y_m \in \mathbb{R}^m$ that minimizes*

$$J(y) = \|\beta e_1 - \overline{H}_m y\|_2 \tag{2.9}$$

   for all $y \in R^m$, where $e_1 = [1, 0, \ldots, 0]^\top$.
   (b) *Compute $z^{(m)} = z^{(0)} + V_m y_m$.*

(4) *Restart: If satisfied stop, else set $z^{(0)} \leftarrow z^{(m)}$ and goto (2).*

The implication from (2.7) to (2.9) can be found in [15]. Note that in (2.8) the matrix-vector multiplication is performed via

$$A v_k = \begin{bmatrix} H'(w_i) \\ t_{i-1}^\top \end{bmatrix} \cdot v_k = \begin{bmatrix} H'(w_i)\, v_k \\ t_{i-1}^\top\, v_k \end{bmatrix}. \tag{2.10}$$

Since the evaluation of $H'(w_i)v_k$ may be costly for large scale problems, an inexpensive approximation may be made by using the central difference formula (see [8,9])

$$H'(w_i)\, v_k = (2\varepsilon)^{-1}(H(w_i + \varepsilon\, v_k) - H(w_i - \varepsilon\, v_k)) + O(\varepsilon^2) \tag{2.11}$$

or the forward difference formula

$$H'(w_i)\, v_k = \varepsilon^{-1}(H(w_i + \varepsilon\, v_k) - H(w_i)) + O(\varepsilon) \tag{2.12}$$

for an appropriate discretization step $\varepsilon\, \|v_k\|$. It seems that one may choose ε in a flexible way, see [9]. A local convergence theory for the forward difference GMRES algorithm was given in [17]. A similar result also holds if the forward difference is replaced by the central difference. Our numerical experiments show that the finite difference GMRES algorithms converge slowly and sometimes fail to converge near the bifurcation point.

The solution of (2.9) is obtained by performing a QR decomposition of $\overline{H}_m$ via Givens rotations, which is updated at each step of the Arnoldi process. With this implementation the residual norm of the approximate solution $z^{(m)}$ can be obtained without additional cost, see [15] for details. Because of the drawback of the finite difference GMRES algorithm mentioned above, one may evaluate the Jacobian matrix explicitly. Therefore, the incomplete LU factorization can be used to obtain the preconditioner, see [8,14,18] and the discussion in Section 2.4 given below.

2.3. Solving Minimization Problems for Correctors

From (2.1) it is obvious that one may obtain the solution curves by solving the minimization problem

$$\varphi(y) := \frac{1}{2}\, \|L^{-1} H(y)\|_2^2. \tag{2.13}$$

Here, L is a nonsingular preconditioner yet to be determined. One may solve (2.13) for correctors by exploiting a global strategy presented by Dennis and Schnabel [19], where the search direction is determined by GMRES methods, see [13,17]. Since the predictor points are close to the solution curve, it is obvious that we will obtain a modified Newton corrector if this global strategy is incorporated in the context of continuation methods. These hybrid methods will be briefly discussed as follows.

Let $p \in \mathbb{R}^{N+1}$ and $\sigma \in \mathbb{R}$. Define $h(\sigma) = \varphi(y + \sigma p)$. Then

$$h'(\sigma) = \varphi'(y + \sigma p) = \nabla\varphi\,(y + \sigma p)^\top p, \tag{2.14}$$

where $\varphi'(y) = \left(\frac{\partial\varphi}{\partial y_1}(y), \ldots, \frac{\partial\varphi}{\partial y_{N+1}}(y)\right) := \nabla\varphi(y)^\top$ with $\nabla\varphi(y)$ denoting the gradient of φ. It is easy to check that

$$\nabla\varphi(y) = H'(y)^\top (LL^\top)^{-1} H(y)$$

is orthogonal to the solution manifold $H^{-1}(0)$. Note that in [10], a secant-conjugate gradient algorithm is proposed, where $\nabla\varphi(y)$ is used as the search direction. From (2.14) it is obvious that a descent direction for φ at the current approximation y is any direction $p \in \mathbb{R}^{N+1}$ such that

$$h'(0) = \nabla\varphi(y)^{\mathsf{T}} p = H(y)^{\mathsf{T}} (LL^{\mathsf{T}})^{-1} H'(y)\, p < 0.$$

For such a direction p there exists a certain $\sigma_0 > 0$ such that

$$\varphi(y + \sigma p) < \varphi(y), \qquad \forall\, 0 \le \sigma \le \sigma_0,$$

see, e.g., [20]. Now let $\bar{z}$ be an approximate solution of (2.6), which is provided either by the linear or nonlinear GMRES methods. The corresponding residual $\bar{r}$ is given by

$$\begin{aligned} \bar{r} := \begin{bmatrix} \bar{r}' \\ \bar{r}_{N+1} \end{bmatrix} = b - A\bar{z} &= \begin{bmatrix} -H(y) \\ 0 \end{bmatrix} - \begin{bmatrix} H'(y) \\ t^{\mathsf{T}} \end{bmatrix} \bar{z} \\ &= \begin{bmatrix} -H(y) - H'(y)\,\bar{z} \\ -t^{\mathsf{T}} z \end{bmatrix} \end{aligned} \tag{2.15}$$

with $\bar{r}' \in \mathbb{R}^N$ and $\bar{r}_{N+1} \in \mathbb{R}$. Then

$$H(y)^{\mathsf{T}} (LL^{\mathsf{T}})^{-1} H'(y)\,\bar{z} = -H(y)^{\mathsf{T}} (LL^{\mathsf{T}})^{-1} H(y) - H(y)^{\mathsf{T}} (LL^{\mathsf{T}})^{-1} H'(y)\,\bar{r}'.$$

Thus, $\bar{z}$ will be a descent direction for φ at y whenever

$$|H(y)^{\mathsf{T}} (LL^{\mathsf{T}})^{-1} H'(y)\,\bar{r}'| < \|L^{-1} H(y)\|_2^2.$$

The following results may be easily obtained from [13].

PROPOSITION 2.1. *Let y be the current Newton-GMRES iterate, 0 is a regular value of $H = H(y)$. Let $z^{(m)} = V_m y_m$ be the direction provided by the GMRES method assuming $z^{(0)} = 0$. If $z^{(m)} \neq 0$, then $z^{(m)}$ is a descent direction for H at y.*

Instead of using the stepsize selection strategy presented by Dennis and Schnabel [19] or Glowinski *et al.* [21], we will incorporate an inexpensive inexact line search given in [8] to our algorithm. More precisely, applying the Taylor expansion to $h(\sigma) = \varphi(y + \sigma p)$, we have

$$\varphi(y + \sigma p) = \varphi(y) + \sigma\, \varphi(y)'\, p + \frac{1}{2}\sigma^2 p^{\mathsf{T}}\, \nabla\varphi(y)'\, p + O(\sigma^3 \|p\|^3). \tag{2.16}$$

Denoting the exact line search solution to

$$\min_{\sigma \ge 0} \varphi(y + \sigma p)$$

by $\sigma_{\min}$, then from (2.16) we have

$$\sigma_{\min} = \frac{-\varphi'(y)\, p}{p^{\mathsf{T}}\, \Delta\varphi(y)'\, p} + O(\sigma_{\min}^2 \|p\|^3), \tag{2.17}$$

where $\Delta\varphi(y)' = H'(y)^{\mathsf{T}} (LL^{\mathsf{T}})^{-1} H'(y) + O(\|H(y)\|)$. Thus, we obtain the approximation

$$\bar{\sigma} := \frac{(L^{-1} H(y))^{\mathsf{T}} (L^{-1} H'(y)\, p)}{\|L^{-1} H'(y)\, p\|_2^2} \tag{2.18}$$

with relative truncation error

$$\frac{|\bar{\sigma} - \sigma_{\min}|}{|\bar{\sigma}|} = O(\|H(y)\|).$$

Now we are ready to describe the secant-line search backtrack algorithm.

ALGORITHM 2.2. *Secant-Line Search Backtrack.*

(1) *Input:*
$y \in R^{N+1}$ {*approximate point on* $H^{-1}(0)$}
$t \in R^{N+1}$ {*approximation to tangent vector*}
$h > 0$; {*step length*}
(2) *Predictor step*
$v := y + ht$
(3) *Corrector step*
Solve (2.6) by Algorithm 2.1 to obtain $\bar{z}$;
Set $w := v + \bar{\sigma}\bar{z}$, *where* $\bar{\sigma}$ *is obtained via (2.18);*
until convergence.
(4) *Adapt stepsize* $h > 0$;
$t := (w - y)/\|w - y\|$;
$y := w$ *and goto (2) until traversing is stopped.*

Note that in Algorithm 2.2 (3) is nothing but the general Newton corrector whenever $\bar{\sigma} = 1$ at each corrector step.

2.4. Preconditioning Techniques

For simplicity, we will only deal with preconditioning techniques for (2.13). We remark that similar techniques may be applied to both linear and nonlinear conjugate gradient type methods, see, e.g., [8,9].

If we choose $L = I$, the (2.13) is the general minimization problem. Three possible choices for L are:

(1) $L = B$, where B is the matrix corresponding to the linear part of the nonlinear system of equations, see [13]. In the case of semilinear elliptic eigenvalue problems, B is the discretized matrix corresponding to $-\Delta$, see [9].
(2) $L = D$, that is, preconditioned by scaling, see [9] and the references cited therein.
(3) $L = D_x H(y)$, i.e., the preconditioner is updated at each outer continuation step, where y is the current approximation solution to $H^{-1}(0)$, see [9].

Note that in [8], L is chosen so that $L \approx D_x H(y)$. Actually, our numerical results in [9] showed that the preconditioners (3) are not superior to (2), where the GMRES was used as a linear solver for (2.6). By using (2) as the preconditioner for the secant-conjuate gradient algorithm [8] certain amount of operations on performing Given rotations for the reduction of $LL^{\mathsf{T}} \approx H'(v)\,H'(v)^{\mathsf{T}}$ clearly can be reduced. We remark here that Irani *et al.* [22] also studied preconditioned conjugate gradient methods for curve-tracking problems.

3. SEMILINEAR ELLIPTIC EIGENVALUE PROBLEMS

In this section, we will discuss the basic theory and finite difference approximations of the following semilinear elliptic eigenvalue problems with Neumann boundary conditions

$$\begin{aligned} \Delta u + \lambda f(u) &= 0 \qquad \text{in } \Omega = (0,1)^2, \\ \frac{\partial u}{\partial n} &= 0 \qquad \text{on } \partial\Omega. \end{aligned} \tag{3.1}$$

Here, f is a smooth odd map in u which satisfies $f(0) = 0$, $f'(0) = 1$ and $f'''(0) \neq 0$, and $\frac{\partial}{\partial n}$ denotes the normal derivative.

3.1. Basic Theory

Consider the following 1D and 2D linear eigenvalue problems with Neumann boundary conditions

$$\begin{aligned} u'' + \lambda u &= 0 \qquad \text{in } \Omega = (0,1), \\ u'(0) = u'(1) &= 0; \end{aligned} \tag{3.2}$$

and

$$\begin{aligned} \Delta u + \lambda u = 0 \qquad & \text{in } \Omega = (0,1)^2, \\ \frac{\partial u}{\partial n} = 0 \qquad & \text{on } \partial\Omega. \end{aligned} \tag{3.3}$$

Without loss of generality, we will treat (3.3). It is obvious that the eigenfunctions u of (3.3) satisfy for all $v \in H^1(\Omega)$

$$\int_\Omega (\nabla u \, \nabla v)\, dx\, dy = -\lambda \int_\Omega u\, v\, dx\, dy. \tag{3.4}$$

A nonzero function $u \in H^1(\Omega)$ is called a generalized eigenfunction of (3.3) if there is an eigenvalue λ corresponding to u such that u satisfies (3.4) for all $v \in H^1(\Omega)$, see [23]. Define an inner product in $H^1(\Omega)$ by

$$(u,v) = \int_\Omega u\, v\, dx\, dy \quad \text{and} \quad a(u,v) = \int_\Omega \nabla u\, \nabla v\, dx\, dy,$$

respectively.

The following results may be easily obtained from [23].

Lemma 3.1. *There is a bounded linear operator $T : L_2(\Omega) \to H^1(\Omega)$ such that for all $v \in H^1(\Omega)$ the following relation holds:*

$$(u,v) = a(Tu, v).$$

the operator T has an inverse T^{-1}. If $T : H^1(\Omega) \to H^1(\Omega)$, then it is self-adjoint, positive and completely continuous.

Theorem 3.2. *The eigenvalues λ_i for the Laplacian $-\Delta$ in (3.3) are real and $\lambda_i \to \infty$ as $i \to \infty$. Furthermore, $\lambda_i \geq 0 \; \forall\, i = 1,2,3,\ldots$ and 0 is a simple eigenvalue with corresponding generalized eigenfunction equal to 1. The generalized eigenfunctions for (3.3) constitute an orthonormal basis for $L_2(\Omega)$.*

Now we will discuss the solution branches of (3.1) bifurcating from the trivial solution curve $\{(0,\lambda) \mid \lambda \in R\}$. Rewriting (3.1) as

$$\begin{aligned} F(u,\lambda) := \Delta u + \lambda f(u) = 0 \qquad & \text{in } \Omega = [0,1]^2, \\ \frac{\partial u}{\partial n} = 0 \qquad & \partial\Omega, \end{aligned}$$

the Frechet derivative of F at $(0,\lambda)$ is given by

$$F'(0,\lambda) = (D_u F(0,\lambda), D_\lambda F(0,\lambda)) = (\Delta + \lambda I, 0).$$

The bifurcation points of (3.1) on the trivial solution curve have the form $(0, \lambda_{m,n})$, where $\lambda_{m,n}$ is given in (3.6). For $m \neq n$, we have

$$\dim N(F_u(0,\lambda_{m,n})) = \rho, \quad \dim N(F'(0,\lambda_{m,n})) = 1 + \rho, \qquad \rho \geq 1,$$

where $N(L)$ denotes the null space of a bounded linear operator L, and ρ is the multiplicity of $\lambda_{m,n}$. Thus, $(0,\lambda_{m,n})$ is a corank ρ bifurcation point, see [2] for details. The following result is given in [2].

Theorem 3.3. *At a corank ρ bifurcation point $(0,\lambda_{m,n})$, (3.1) has exactly $(3^\rho - 1)/2$ different nontrivial solution curves. Moreover, if $f'''(0) > 0$, these solution curves are stable. Conversely, for $f'''(0) < 0$, these solution curves are unstable.*

It is well known that the eigenvalues and generalized eigenfunctions of (3.2) and (3.3) are given by

$$\begin{aligned} \lambda_m &= m^2\pi^2, \\ u_m(x) &= \pm\cos m\pi x, \qquad m = 0,1,2\ldots \end{aligned} \tag{3.5}$$

and

$$\begin{aligned} \lambda_{m,n} &= (m^2+n^2)\,\pi^2, \\ u_{m,n}(x,y) &= \pm\cos m\pi x \cdot \cos n\pi y, \qquad m,n = 0,1,2,\ldots, \end{aligned} \tag{3.6}$$

respectively.

3.2. Finite Difference Approximation

We will show that the discretized matrix and eigenvectors of (3.3) may be obtained from the counterparts of (3.2) via tensor products.

Let $A = (a_{ij})$, $B = (b_{ij})$ be real m by n, and p by q matrices, respectively. The matrix tensor producut of A and B, denoted by $A \otimes B$, is a real mp by nq matrix, and defined by

$$A \otimes B = \begin{bmatrix} a_{11}B & a_{12}B & \dots & a_{1n}B \\ a_{21}B & a_{22}B & \dots & a_{2n}B \\ \vdots & \vdots & \ddots & \vdots \\ a_{m1}B & a_{m2}B & \dots & a_{mn}B \end{bmatrix}.$$

Note that in general $A \otimes B \neq B \otimes A$ unless $A = 0$ or $B = 0$, see [24].

In the method of standard three-point central difference approximation with mesh points $x_i = ih$, $i = 0, 1, \dots, N$, where $h = 1/N$ is the uniform meshsize on $(0, 1)$, the discretized matrix corresponding to the second order differential operator in (3.2) is $A_h^{(1)} \in \mathbb{R}^{(N+1)\times(N+1)}$, which is given by

$$A_h^{(1)} = \frac{1}{h^2} \begin{bmatrix} 2 & -2 & & & 0 \\ -1 & 2 & -1 & & \\ & \ddots & \ddots & \ddots & \\ & & -1 & 2 & -1 \\ 0 & & & -2 & 2 \end{bmatrix}.$$

The eigenpairs of $A_h^{(1)}$ are

$$\begin{aligned} \mu_m &= 2N^2\left(1 - \cos\frac{m\pi}{N}\right), \\ U_m(x_i) &= \pm\cos\frac{m_i\pi}{N}, \qquad 0 \le m,\ i \le N. \end{aligned} \tag{3.7}$$

Similarly let $x_i = ih$, $y_j = jh$, $0 \le i,\ j \le N$ be the mesh on $[0, 1]^2$, where $h = 1/N$ is the uniform meshsize on the x- and y-axis for some positive integer N. The five-point central difference analogue of (3.5) is

$$\begin{aligned} -\Delta_h U &= \mu U \qquad && \text{in } \Omega = [0, 1]^2, \\ \frac{\partial U}{\partial n} &= 0 && \text{on } \partial\Omega, \end{aligned} \tag{3.8}$$

where Δ_h is the central difference operator corresponding to the Laplacian Δ. The discretized matrix corresponding to $-\Delta_h$ is $A_h^{(2)} \in \mathbb{R}^{(N+1)^2\times(N+1)^2}$, where

$$A_h^{(2)} = \frac{1}{h^2} \begin{bmatrix} A_{N+1} & -2I_{N+1} & & & 0 \\ -I_{N+1} & A_{N+1} & -I_{N+1} & & \\ & \ddots & \ddots & \ddots & \\ & & -I_{N+1} & A_{N+1} & -I_{N+1} \\ 0 & & & -2I_{N+1} & A_{N+1} \end{bmatrix}, \tag{3.9}$$

and $A_{N+1}, I_{N+1} \in \mathbb{R}^{(N+1)\times(N+1)}$ with

$$A_{N+1} = \begin{bmatrix} 4 & -2 & & & 0 \\ -1 & 4 & -1 & & \\ & \ddots & \ddots & \ddots & \\ & & -1 & 4 & -1 \\ 0 & & & -2 & 4 \end{bmatrix}$$

and I_{N+1} is the identity matrix. Note that $A_h^{(2)}$ is a banded nonsymmetric matrix with band width $\omega = 2 \cdot (N+1) + 1$.

The eigenpairs of $A_h^{(2)}$ are

$$\begin{aligned} \mu_{m,n} &= 2N^2\left(2 - \cos\frac{m\pi}{N} - \cos\frac{n\pi}{N}\right), \\ U_{m,n}(x_i, y_j) &= \pm\cos\frac{m_i\pi}{N} \cdot \cos\frac{n_j\pi}{N}, \end{aligned} \tag{3.10}$$

for $0 \le m, n, p, i \le N$. Here, (x_i, y_j) denotes the position of the node in or on $[0,1]^2$.

From the formulae derived above , one may easily check that

$$\begin{aligned} \mu_{m,n} &= \mu_m + \mu_n, \\ A_h^{(2)} &= A_h^{(1)} \otimes I_{N+1} + I_{N+1} \otimes A_h^{(1)}, \\ U_{m,n} &= U_m \otimes U_n. \end{aligned}$$

Here $A_h^{(1)}$, μ_m, μ_n, U_m, U_n and $A_h^{(2)}$, $\mu_{m,n}$, $U_{m,n}$ are defined in (3.3), (3.4), and (3.9), (3.10), respectively. The results given above clearly can be extended to the 3D problem.

For example, let $A_h^{(3)}$ be the discretized matrix corresponding to the 3D Laplacian Δ, $\mu_{m,n,p}$ and $U_{m,n,p}$ be the eigenvalues and corresponding eigenvector. Then, we have

$$\begin{aligned} \mu_{m,n,p} &= \mu_m + \mu_n + \mu_p, \\ A_h^{(3)} &= A_h^{(1)} \otimes I_{N+1} \otimes I_{N+1} + I_{N+1} \otimes A_h^{(1)} \otimes I_{N+1} + I_{N+1} \otimes I_{N+1} \otimes A_h^{(1)}, \\ U_{m,n,p} &= U_m \otimes U_n \otimes U_p. \end{aligned}$$

Furthermore, similar results hold if Neumann boundary conditions are replaced either by Dirichlet or mixed type boundary conditions, respectively.

4. NUMERICAL RESULTS

The numerical methods described in Section 2 will be used to trace the solution curves of (1.2) and the thin plate buckling problem. Throughout our numerical experiments the stopping criterion for corrector step is 5×10^{-4}. The perturbation vector d is chosen so that $\|d\|_\infty = 9 \times 10^{-4}$. The computations were performed on a Vax 9210 at National Chung-Hsing University.

EXAMPLE 4.1. STABLE BIFURCATIONS. For convenience we rewrite (1.2) as follows:

$$\begin{aligned} \Delta u + \lambda \sin hu &= 0 \qquad \text{in } \Omega = [0,1]^2, \\ u &= 0 \qquad \text{on } \partial\Omega. \end{aligned} \tag{4.1}$$

One can easily check that $f(u) = \sin hu$ satisfies all of the requirements for $f(u)$ given in Section 1. Moreover, the bifurcations of (4.1) are stable and turn to the left. (4.1) is discretized by a standard five-point central difference formula with various uniform meshsizes $h = 1/(K+1) = \frac{1}{4}, \frac{1}{5}, \frac{1}{6}, \frac{1}{10}, \frac{1}{20}$, respectively, see [25]. The eigenvalues of the central difference analogue of (4.1) are given by (see [26])

$$\mu_{p,q} = 4(K+1)^2\left[\sin^2\left(\frac{\pi}{2} \cdot \frac{p}{K+1}\right) + \sin^2\left(\frac{\pi}{2} \cdot \frac{q}{K+1}\right)\right], \qquad 1 \le p, \quad q \le K$$

with corresponding eigenvectors $U_{p,q}$.

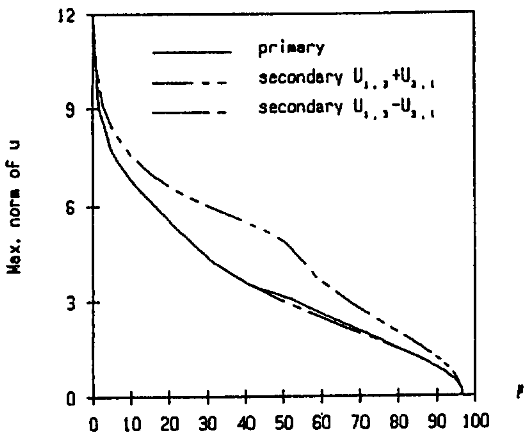

Figure 1. $f(u) = \sinh u$, solution branches bifurcating from $\mu_{1,3} \cong 97.044$.

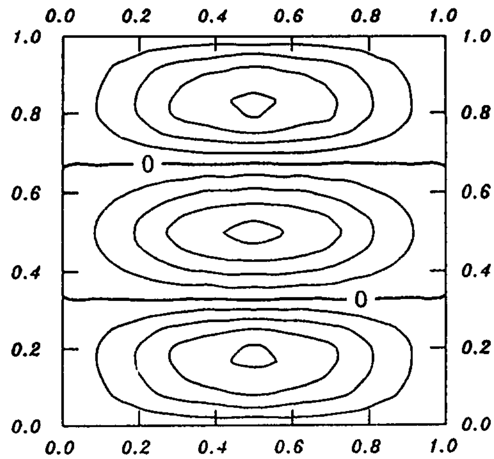

Figure 2. $f(u) = \sinh u$, contour of the primary state at $\mu = 87.28$ bifurcating from $\mu_{1,3}$.

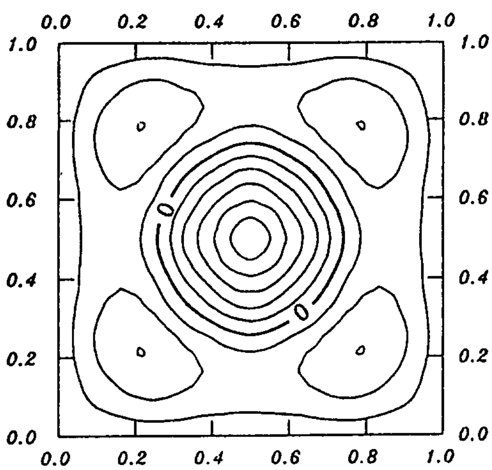

Figure 3. $f(u) = \sinh u$, contour of the secondary state at $\mu = 87.27$ bifurcating from $\mu_{1,3}$.

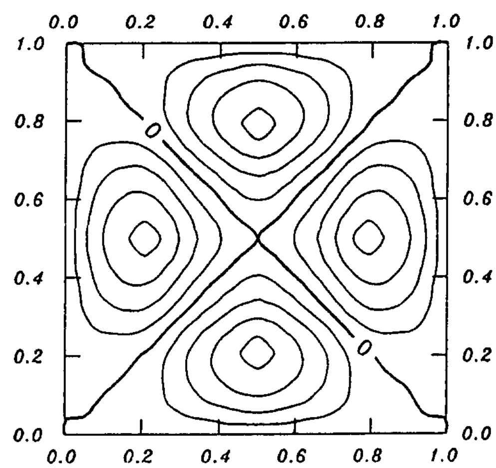

Figure 4. $f(u) = \sinh u$, contour of the secondary state at $\mu = 87.28$ bifurcating from $\mu_{1,3}$.

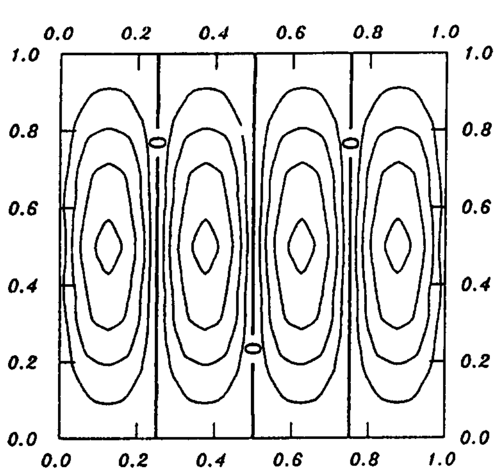

Figure 5. $f(u) = \sinh u$, contour of the primary state at $\mu = 150.58$ bifurcating from $\mu_{4,1}$.

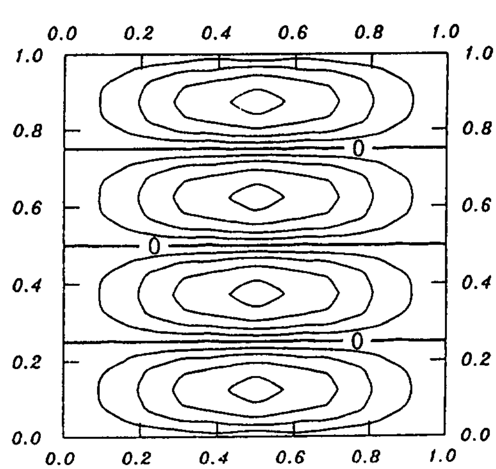

Figure 6. $f(u) = \sinh u$, contour of the primary state at $\mu = 150.58$ bifurcating from $\mu_{1,4}$.

We first trace the solution curves bifurcating from $(0,\mu_{1,2})$. It is clear that $(0,\mu_{1,2})$ is a corank 2 bifurcation point. We obtain two primary states (or rectangular solutions) $U_{1,2}$, $U_{2,1}$, and two secondary states (or triangular solutions) $U_{1,2}+U_{2,1}$, $U_{1,2}-U_{2,1}$ bifurcating from $(0,\mu_{1,2})$, respectively. This agrees with the result of Theorem 3.3. We also observe that there is no other bifurcation on these four solution curves. The contours of these four solution curves were given in [25].

Next, we trace the solution curve bifurcating from $(0,\mu_{2,2})$. Since $(0,\mu_{2,2})$ is a corank 1 bifurcation point, there is only one primary state bifurcating from it. However, there is a secondary bifurcation on the primary state which is far away from the trivial solution. This secondary state may be obtained by numerical methods or physical experiments. The contours of both the primary and secondary states were also given in [25].

Figure 1 shows the solution branches of two primary and two secondary states bifurcating from $\mu_{1,3} \cong 97.044$, where $h = 0.05$ is used. Note that the maximum norms of the two secondary states are different. Figure 2 shows the contour of the primary state $U_{3,1}$ at $\mu = 87.28$. Figures 3 and 4 show the contours of the secondary states $U_{1,3} + U_{3,1}$ and $U_{1,3} - U_{3,1}$ with corresponding nodal lines a circle and two diagonals, respectively, see [1]. This agrees with the result of Theorem 3.3 again. It is obvious that the solution $U_{1,3}+U_{3,1}$ is invariant under the action of the dihedral group D_4, and $U_{1,3} - U_{3,1}$ is invariant under the action of a subgroup of $D_4 \times Z_2$ which is isomorphic to D_4, see [1].

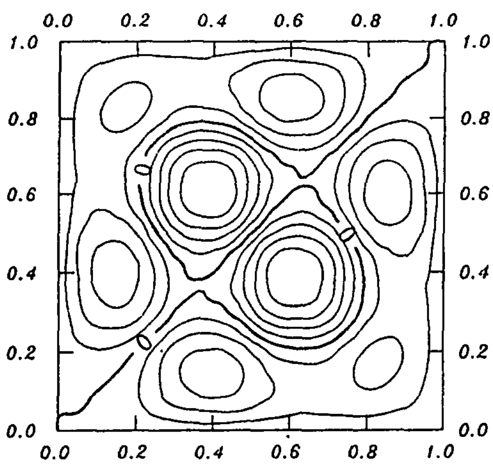

Figure 7. $f(u) = \sin hu$, contour of the secondary state at $\mu = 150.58$ bifurcating from $\mu_{1,4}$.

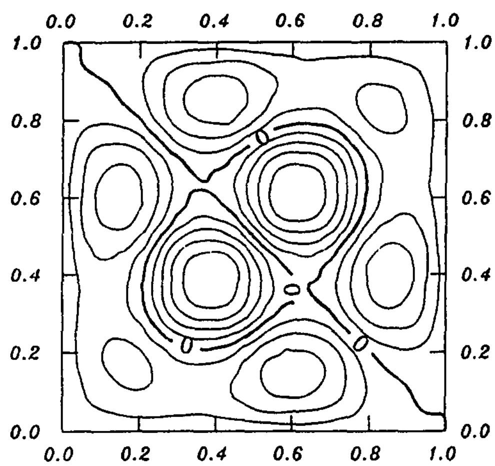

Figure 8. $f(u) = \sin hu$, contour of the secondary state at $\mu = 150.58$ bifurcating from $\mu_{4,1}$.

There are four nontrivial solution branches bifurcating from $\mu_{1,4} \cong 162.64$. Figures 5–8 show the contours of two primary states $U_{1,4}$, $U_{4,1}$, and two secondary states $U_{1,4} + U_{4,1}$, $U_{1,4} - U_{4,1}$, respectively. The nodal lines of $U_{1,4} + U_{4,1}$ and $U_{1,4} - U_{4,1}$ are exactly the same as those given in [1] which are obtained by group theoretic methods.

EXAMPLE 4.2. UNSTABLE BIFURCATIONS. Consider the thin plate buckling problem

$$\begin{aligned} \Delta u + \lambda \sin u &= 0 \qquad \text{in } \Omega = [0,1] \times [0,1+\delta], \\ u &= 0 \qquad \text{on } \partial\Omega. \end{aligned} \tag{4.2}$$

For the unperturbed problem $\delta = 0$ some numerical results concerning the primary and secondary states of (4.2) were given in [6,7]. Now, (4.2) is discretized by a standard five-point central difference formula with various uniform meshsizes $h = \frac{1}{4}, \frac{1}{5}, \frac{1}{7}, \frac{1}{8}, \frac{1}{10}, \frac{1}{20}$, respectively, where both the unperturbed problem and perturbed problem with $\delta = 0.1$ and $\delta = 0.01$ are tested.

First, we trace nontrivial solution bifurcating from the bifurcation point $(0,\mu_{1,2})$. We found four nontrivial solutions branching from this bifurcation point only when the meshsize $h = \frac{1}{4}$ is used, see [7]. For $h > \frac{1}{4}$, we just got two rectangular solutions branching from this bifurcation

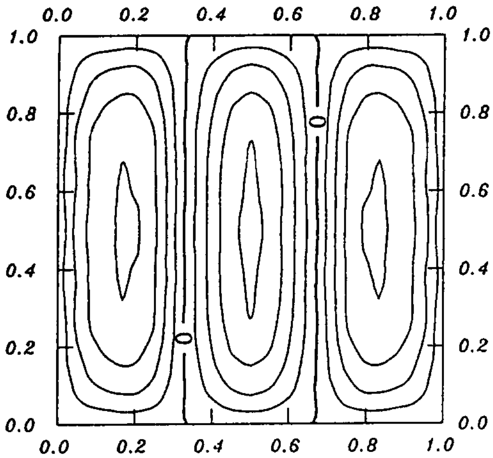

Figure 9. $f(u) = \sin u$, contour of the primary state at $\mu = 173.58$ bifurcating from $\mu_{3,1}$.

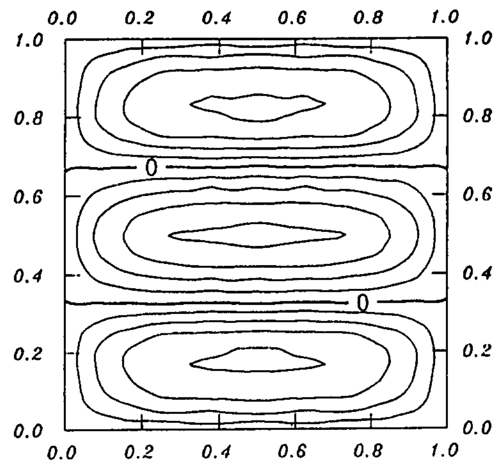

Figure 10. $f(u) = \sin u$, contour of the primary state at $\mu = 173.58$ bifurcating from $\mu_{1,3}$.

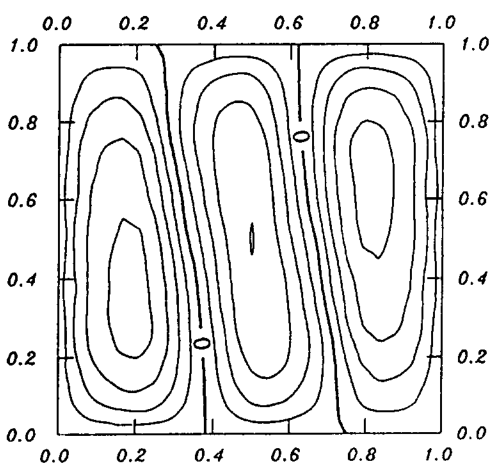

Figure 11. $f(u) = \sin u$, contour of the secondary state at $\mu = 173.59$ bifurcating from $\mu_{3,1}$.

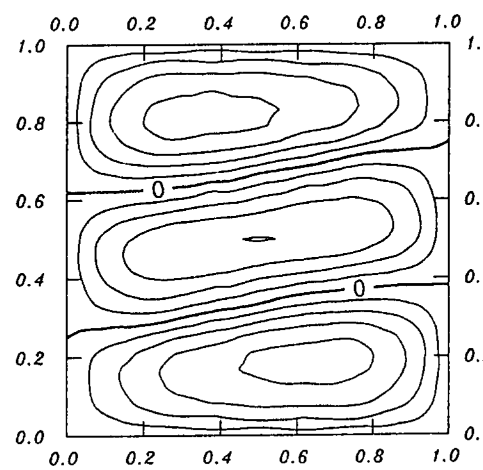

Figure 12. $f(u) = \sin u$, contour of the secondary state at $\mu = 173.59$ bifurcating from $\mu_{1,3}$.

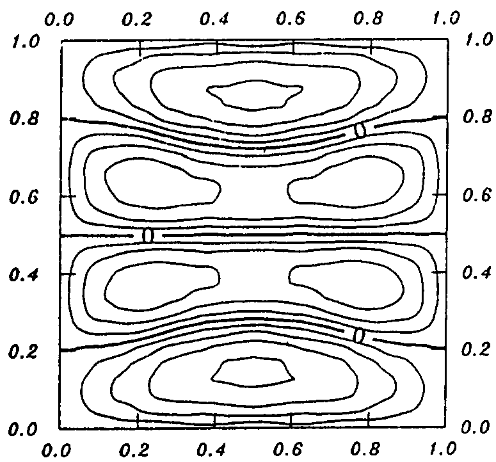

Figure 13. $f(u) = \sin u$, contour of the secondary state at $\mu = 273.04$ bifurcating from $\mu_{4,1}$.

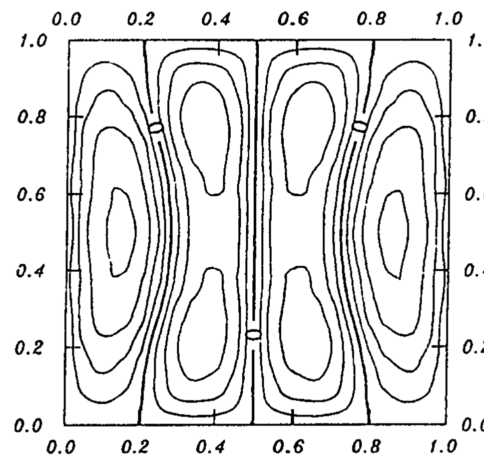

Figure 14. $f(u) = \sin u$, contour of the secondary state at $\mu = 273.05$ bifurcating from $\mu_{1,4}$.

Table 1. Bifurcations for (4.2), $\delta = 0.1$.

N		3^2			4^2		
		primary	secondary	tertiary	primary	secondary	tertiary
$\lambda_{11} = 18.026$	μ_{11}	17.119	no	no	17.441	no	no
$\lambda_{12} = 42.496$	μ_{12}	35.819	(49.68,50.08)	no	38.102	(56.33,56.72)	(68.65,69.05)
							(114.6,116.2)
			(77.64,78.04)	no			(134.7,135.6)
$\lambda_{21} = 47.635$	μ_{21}	39.746	(71.27,71.67)	no	42.441	(50.92,51.31)	no
						(64.38,64.77)	(71.52,71.92)
$\lambda_{22} = 72.105$	μ_{22}	58.446	(79.05,79.45)	no	63.102	(80.65,81.05)	(82.78,83.57)
							(103.9,104.3)
							(140.6,141.0)
						(85.03,85.43)	(105.7,105.9)
							(113.5,113.7)
						(108.6,109.0)	(116.1,116.5)

Table 2. Bifurcations for (4.2), $\delta = 0.01$.

N		3^2			4^2		
		primary	secondary	tertiary	primary	secondary	tertiary
$\lambda_{11} = 19.545$	μ_{11}	18.56	no	no	18.91	no	no
$\lambda_{12} = 48.570$	μ_{12}	40.7421	(47.02,47.22)	no	43.418	(64.96,65.76)	(75.80,76.20)
							(120.9,122.4)
			(81.52,81.92)	no			(146.4,147.9)
$\lambda_{21} = 49.154$	μ_{21}	41.188	(80.72,81.12)	no	43.91	(45.24,45.61)	(92.57,92.97)
							(100.9,101.9)
						(65.98,66.38)	(75.99,76.79)
							(119.9,120.7)
							(147.1,147.9)
$\lambda_{22} = 78.179$	μ_{22}	63.369	(84.72,85.12)	no	68.418	(89.75,89.85)	no
						(90.25,90.35)	(112.7,113.1)
							(134.2,135.0)
						(118.0,118.3)	(125.9,126.7)

point. At each primary state there is a secondary bifurcation point on it which is away from the trivial solution. Furthermore, if we decrease the meshsize from $h = \frac{1}{4}$ to $h = \frac{1}{20}$, then we found that the nodal lines of the secondary states vary gradually from a diagonal to a curve which is a slight twist of the line segment $x = \frac{1}{2}$ or $y = \frac{1}{2}$, see the graphs given in [7].

Next, we trace nontrivial solution branching from $(0, \mu_{2,2})$. The contours of the primary and secondary states were given in [7] where $h = \frac{1}{7}$ was used. For $h = \frac{1}{10}$ and $h = \frac{1}{20}$ the contours of the secondary states are similar to the one with $h = \frac{1}{7}$ is used. But the location of the secondary bifurcation points varies with respect to different mesh sizes. Figures 9 and 10 show the contours of the primary states branching from $\mu_{1,3} \cong 97.044$ where the nodal lines are parallel to the sides of the square. From Figures 2 and 10, one may find that the contours of (4.1) are sharper than those of (4.2). The contours of the secondary states bifurcating from each of the primary states $U_{1,3}$ and $U_{3,1}$ at $\mu = 173.58$ are given in Figures 11 and 12, where the secondary bifurcation points are detected at $\mu \in (163.30, 163.31)$. Figures 13 and 14 represent the contours of the secondary states on each of the primary states $U_{4,1}$ and $U_{1,4}$ bifurcating from $\mu_{1,4} \cong 162.64$, where the secondary bifurcation points are detected at $\mu \in (260.87, 260.91)$. Note that the nodal lines of these two secondary states contain the line segments $y = 0.5$ and $x = 0.5$, respectively.

Tables 1 and 2 list some observations of the primary, secondary and tertiary bifurcations in the perturbed problem with $\delta = 0.1$ and 0.01, respectively.

5. CONCLUSIONS

Based on our numerical experiments given above and in [12], we wish to draw some conclusions concerning stable and unstable bifurcations.

(1) All of the nontrivial solutions branching from a corank ρ stable bifurcation point can be numerically determined. Although we only report numerical experiments for corank 2 bifurcation points, it is obvious that our numerical methods will work for that with corank greater than 2. On the other hand, we only can find nontrivial primary states branching from an unstable bifurcation point. However, the secondary state branching from an unstable primary state also can be numerically traced since their nodal lines are predictable.

(2) The nodal lines of the secondary state at a corank one stable bifurcation point are different from its counterparts at an unstable one, see, e.g., the figures given in [7,25]. Since at a corank $\rho \geq 2$ stable bifurcation point the $(3^\rho - 1)/2 - \rho$ nontrivial solution branches play the role of secondary states, a similar result also holds for corank $\rho \geq 2$ bifurcations.

REFERENCES

1. E.L. Allgower, K. Böhmer and Mei Zhen, A generalized equibranching lemma with applications to $D_4 \times Z_2$ symmetric elliptic problems, Bericht Nr. 9, Fachbereich Mathematik, University of Marburg, (1990).
2. E.L. Allgower, K. Böhmer and M. Zhen, A complete bifurcation scenario for the 2-d nonlinear Laplacian with Neumann boundary conditions on the unit square, *Internat. Ser. Numer. Math.* **97**, Birkhauser, Basel, (1991).
3. D.L. Book, S. Fisher and B.E. McDonald, Steady-state distributions of interacting discrete vortices, *Phys. Rev. Lett.* **27**, 4–8 (1975).
4. P.N. Budden and J. Norbury, A nonlinear elliptic eigenvalue problem, *J. Inst. Maths. Applics.* **24**, 9-33 (1979).
5. P.N. Budden and J. Norbury, Solution branches for nonlinear equilibrium problems—bifurcation and domain perturbations, *IMA J. Appl. Math.* **28**, 109–129 (1982).
6. E.L. Allgower and C.-S. Chien, Continuation and local perturbation for multiple bifurcations, *SIAM J. Sci. Stat. Comput.* **7**, 1265–1281 (1986).
7. C.-S. Chien, Secondary bifurcations in the buckling problem, *J. Comput. Appl. Math.* **25**, 277–287 (1989).
8. E.L. Allgower, C.-S. Chien and K. Georg, Large sparse continuation problems, *J. Comput. Appl. Math.* **26**, 3–21 (1989).
9. E.L. Allgower, C.-S. Chien, K. Georg and C.-F. Wang, Conjugate gradient methods for continuation problems, *J. Comput. Appl. Math.* **38**, 1–16 (1991).
10. E.L. Allgower and K. Georg, *Numerical Continuation: An Introduction*, Springer-Verlag, Berlin, (1990).
11. K. Georg, On tracing an implicitly defined curve by quasi-Newton steps and calculating bifurcation by local perturbation, *SIAM J. Sci. Stat. Comput.* **2**, 35–50 (1981).
12. H.B. Keller, *Lectures on Numerical Methods in Bifurcation Problems*, Springer, Berlin, (1987).
13. P.N. Brown and Y. Saad, Hybrid Krylov subspace methods for nonlinear systems of equations, *SIAM J. Sci. Stat. Comput.* **11**, 450–481 (1990).
14. Y. Saad, Krylov subspace methods on supercomputers, *SIAM J. Sci. Stat. Comput.* **10**, 1200–1232 (1989).
15. Y. Saad and M.H. Schultz, GMRES: A generalized minimal residual algorithm for solving nonsymmetric linear systems, *SIAM J. Sci. Stat. Comput.* **7**, 856–869 (1986).
16. Y. Saad, Krylov subspace methods for solving large unsymmetric linear systems, *Math. Comput.* **37**, 105–126 (1981).
17. P.N. Brown, A local convergence theory for combined inexact-Newton/finite difference projection methods, *SIAM J. Numer. Anal.* **24**, 407–434 (1987).
18. G.H. Golub and C.F. van Loan, *Matrix Computations*, Johns Hopkins University Press, Baltimore, MD, (1989).
19. J.E. Dennis and R.B. Schnabel, *Numerical Methods for Unconstrained Optimization*, Prentice-Hall, Englewood Cliffs, NJ, (1983).
20. J. Stoer and R. Bulirsch, *Introduction to Numerical Analysis*, Springer-Verlag, New York, (1980).
21. R. Glowinski, H.B. Keller and L. Reinhart, Continuation-conjugate gradient methods for the least square solution of nonlinear boundary value problems, *SIAM J. Sci. Stat. Comput.* **6**, 793–832 (1985).

22. K.M. Irani, C.J. Ribbens, H.F. Walker, L.T. Watson and M.P. Kamet, Preconditioned conjugate gradient algorithms for homotopy curve tracking, (preprint), Virginia Polytechnic Institute and State University, (1989).
23. V.P. Mikhailov, *Partial Differential Equations*, (English translation, 1978), Mir Publishers, Moscow, (1976).
24. A.R. Mitchell and R. Wait, *The Finite Element Method in Partial Differential Equations*, John Wiley and Sons, (1978).
25. C.-S. Chien, On some derivative-free continuation methods, In *Proceedings of 10th International Conference on Computing Methods in Applied Sciences and Engineering*, (Edited by R. Glowinski), pp. 679–688, Nova Science Publishers, (1992).
26. E. Isaacson and H. B. Keller, *Analysis of Numerical Methods*, John Wiley, New York, (1965).